

Density-matrix renormalization group for the Berezinskii-Kosterlitz-Thouless transition of the 19-vertex model

Yasushi Honda and Tsuyoshi Horiguchi

Department of Computer and Mathematical Sciences, Graduate School of Information Sciences, Tohoku University, Sendai 980-77, Japan

(Received 11 June 1997)

We embody the density-matrix renormalization-group (DMRG) method for the 19-vertex model on a square lattice in order to investigate the Berezinskii-Kosterlitz-Thouless transition. Elements of the transfer matrix of the 19-vertex model are classified in terms of the total value of arrows in one layer of the square lattice. By using this classification, we succeed in reducing enormously the dimension of the matrix that has to be diagonalized in the DMRG method. We apply our method to the 19-vertex model with the interaction $K=1.0866$ and obtain $c=1.006(1)$ for the conformal anomaly. [S1063-651X(97)03810-5]

PACS number(s): 05.90.+m, 02.70.-c

I. INTRODUCTION

The density-matrix renormalization-group (DMRG) method is developed to obtain eigenvalues of the Hamiltonian matrix for one-dimensional quantum systems [1]. This method enables us to investigate a finite system with a large size by a numerical calculation of matrices, which can be handled within recent computer resources such as memory size and CPU speed. Recently, the DMRG method has been applied to the transfer matrix of classical spin systems [2]. In the both cases of quantum systems and classical systems, each spin variable has a discrete degree of freedom. Therefore, we have matrices with a finite dimension for these finite systems. On the other hand, the dimension of the transfer matrix becomes infinite for a finite system of spins with a continuous degree of freedom such as a classical XY model. Fortunately, it is known that the XY model on a square lattice Λ is translated into a 19-vertex model for which the transfer matrix is described in terms of the realization of arrow variables [3]. An arrow variable takes three discrete states. Hence the 19-vertex model is called a three-state vertex model. We can construct the transfer matrix with a finite dimension for a finite system of the 19-vertex model described by the three-state variables. The 19-vertex model is solved by Zamolodchikov and Fateev [4] in the case that its Boltzmann weights satisfy the Yang-Baxter relation. This exact solution is generalized to the q -state vertex model by Sogo *et al.* [5,6]. When the Yang-Baxter relation is not satisfied, we do not have an exact solution yet for that system. However, it is believed that a critical behavior of the 19-vertex model without frustration belongs to the same universality class as the Berezinskii-Kosterlitz-Thouless (BKT) transition [3,7-9].

The purpose of the present paper is to embody the DMRG method for the 19-vertex model and to show that the dimension of matrices, which are diagonalized in the DMRG method, is reduced enormously by using the ice rule of the 19-vertex model [10]. We obtain a value of the conformal anomaly as $c=1.006(1)$ at $K=1.0866$, which is regarded as the BKT transition point [3]. This value is consistent with a value of c expected at the BKT transition point. On the other

hand, the value of $\eta/2$ appears to be 0.1175(5), which is smaller than the expected value $\frac{1}{8}$ at the BKT transition point. This suggests that the critical value of K for the 19-vertex model is smaller than 1.0866.

In Sec. II we briefly explain the relation between the classical XY model and the 19-vertex model. In Sec. III we explain our method by which we can reduce the dimension of the transfer matrix in the DMRG method. In Sec. IV we show our results and discuss the conformal anomaly and the smallest scaling dimension. Section V is a summary of the present study.

II. 19-VERTEX MODEL

The partition function of the 19-vertex model is derived from that of the XY model. Assigning Boltzmann weights to 19 vertices, the 19-vertex model describes the XY model on a square lattice for each case with frustrations or without frustrations. For spin variables, which take continuous values like classical XY spins or plane rotators, we have a transfer matrix with an infinite dimension even for a finite system. Therefore, the bare XY model cannot be handled by a numerical diagonalization of the transfer matrix. On the other hand, the 19-vertex model is described by discrete variables that express three kinds of arrows. Hence we can make a transfer matrix with a finite dimension and apply the DMRG procedure for a finite system. In order to demonstrate the efficiency of our approach to the BKT transition, we apply it to the 19-vertex model without frustration for which the critical behavior of the usual BKT transition has to be reproduced.

Let us briefly explain the relation between the XY model and the 19-vertex model on a square lattice Λ . The partition function Z_{XY} of the XY model on the square lattice Λ is defined as

$$Z_{XY} = \prod_{k \in \Lambda} \int_{-\pi}^{+\pi} d\theta_k \exp \left\{ K \sum_{\langle i,j \rangle} \cos(\theta_i - \theta_j - A_{ij}) \right\}, \quad (1)$$

where i, j , and k denote site indices, θ_i is an angle of the XY spin at site i , and K is an interaction parameter, respectively. The sum $\sum_{\langle i,j \rangle}$ is taken over all nearest-neighbor pairs of

sites. A bond parameter related to frustration between sites i and j is expressed by A_{ij} . The frustration f is defined in terms of the A_{ij} as

$$f \equiv \frac{1}{2\pi} \sum_P A_{ij}, \quad (2)$$

where the summation \sum_P is taken over an elementary plaquette. If the value of f is a half odd integer, the plaquette has a frustration.

In a region of small parameter K , we expand the exponential function in the partition function for the XY model given in Eq. (1). Hence let us start with the partition function Z ,

$$\begin{aligned} Z &= \prod_{k \in \Lambda} \int_{-\pi}^{+\pi} d\theta_k \prod_{\langle i,j \rangle} \{1 + K \cos(\theta_i - \theta_j - A_{ij})\} \\ &= \prod_{k \in \Lambda} \int_{-\pi}^{+\pi} d\theta_k \prod_{\langle i,j \rangle} \left\{ 1 + \frac{K}{2} \exp\{i(\theta_i - \theta_j - A_{ij})\} \right. \\ &\quad \left. + \frac{K}{2} \exp\{-i(\theta_i - \theta_j - A_{ij})\} \right\}. \end{aligned} \quad (3)$$

The integrand of the partition function Z has the $U(1)$ symmetry as well as that of Z_{XY} . The first term of the integrand on the right-hand side of Eq. (3) is assigned to no arrow in the 19-vertex model, the second term is assigned to an arrow pointing from site i to site j , and the third term is assigned to an arrow pointing from site j to site i . We use the word ‘‘arrow’’ even for the case of no arrow in a bond. Only when the value of arrows going into a site is equal to the value of arrows leaving the site does the weight of the arrow configuration for the site survive after taking integrations with respect to an angle of XY spin at the site. Otherwise the weights of the arrow configurations do not appear in the partition function. In the six-vertex model, we have a similar rule to that mentioned above [10]. That rule is called the ice rule, whose name comes from the property of hydrogen ions in an ice crystal.

The 19 kinds of arrow configurations on vertices are permitted by the ice rule, which is a generalization of the ice rule for the six-vertex model, when we include no arrow on a bond, as shown in Fig. 1. Hereafter we simply say the 19 kinds of vertices instead of the 19 kinds of arrow configurations on vertices. The vertex weight $W(v_i)$ depends on the kind of vertex $v_i \in \{1, 2, \dots, 19\}$ at site i . The value of v_i is determined by a configuration of four arrows as

$$v_i = v_i(\alpha_i, \beta_i, \gamma_i, \delta_i), \quad (4)$$

where α_i , β_i , γ_i , and δ_i denote arrows surrounding site i , as shown in Fig. 2. Let us express an up and a right arrow by $+1$, a down and a left arrow by -1 , and no arrow by 0 , respectively. For instance, $v_i(-1, 0, 0, +1) = 1$, as shown in Fig. 1. The ice rule is described in terms of α_i , β_i , γ_i , and δ_i as

$$\alpha_i - \beta_i - \gamma_i + \delta_i = 0. \quad (5)$$

Using the weights for 19 vertices, we can describe the partition function Z as

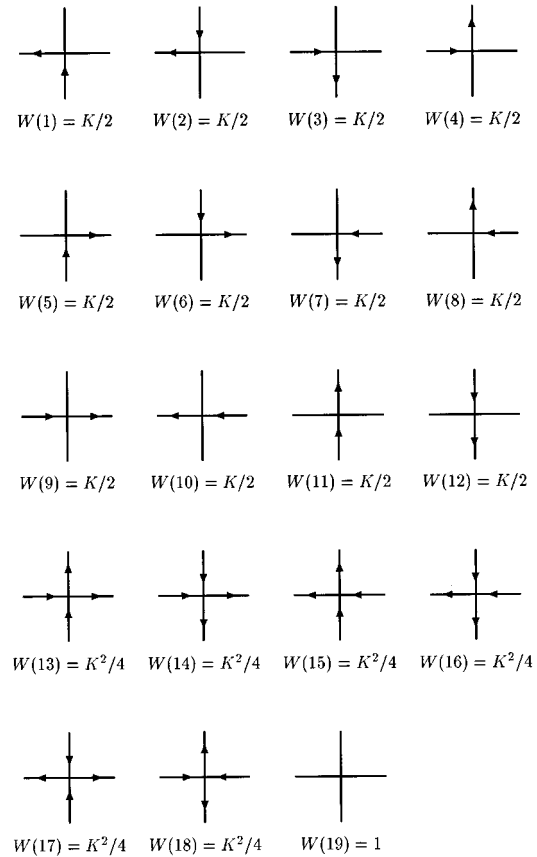


FIG. 1. Nineteen vertices permitted by the ice rule generalized to include no arrow on a bond.

$$Z = \sum'_{\{v_i\}} \prod_{i \in \Lambda} W(v_i), \quad (6)$$

where the summation is taken over all permitted configurations of the vertex on the lattice Λ .

III. DENSITY-MATRIX RENORMALIZATION-GROUP METHOD WITH RESTRICTIONS ON THE TOTAL VALUE OF ARROWS

Because there exists the ice rule for the 19-vertex model, the transfer matrix, by which the partition function Z is expressed, becomes a block-diagonal form. This block-diagonal form is obtained in terms of classification by the

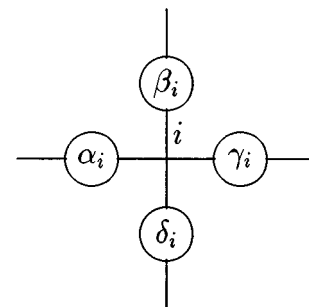


FIG. 2. Four arrows surrounding a site i .

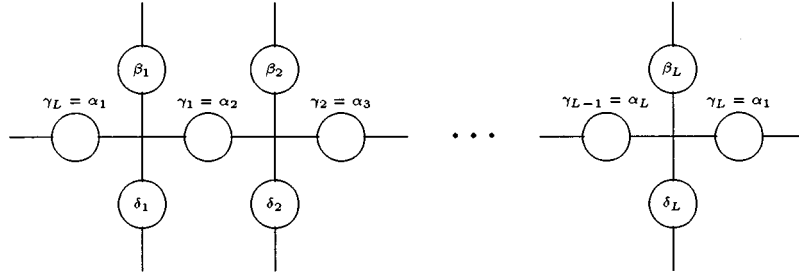


FIG. 3. One layer that corresponds to the transfer matrix. The value of arrows going into the layer is equal to the number of those leaving the layer. When a bond is shared by two vertices the summation for the variable on the bond is taken.

value of arrows going into one layer corresponding to the transfer matrix. The layer with length L is shown in Fig. 3; L is the width of the system. We consider the system under periodic boundary conditions without frustration in this and the following sections.

From the ice rule shown in Eq. (5) we have

$$\sum_{i=1}^L (\alpha_i - \beta_i - \gamma_i + \delta_i) = 0. \quad (7)$$

Because of the relations

$$\gamma_i = \alpha_{i+1} \quad (1 \leq i \leq L), \quad (8)$$

$$\alpha_{L+1} = \alpha_1, \quad (9)$$

Eq. (7) becomes

$$\sum_{i=1}^L \beta_i = \sum_{i=1}^L \delta_i. \quad (10)$$

Here we note that Eq. (9) comes from the periodic boundary conditions. The relation given by Eq. (10) is a conservation law of the total value of arrows. Let us define the total value of arrows N in one layer as

$$N \equiv \sum_{i=1}^L \beta_i. \quad (11)$$

Now the whole transfer matrix of the 19-vertex model is classified by N and hence has a block-diagonal form. We will explain this in detail in the following.

By using the property (10), we reduce the number of calculations in the DMRG method. We apply the infinite system method of the DMRG framework to the 19-vertex model. In addition to the vertex weight $W(v_i)$ whose values are provided in Fig. 1, we define a renormalized weight $W^{(r)}(v_i^{(r)})$, where $v_i^{(r)}$ is a renormalized vertex and r is the number of renormalizations. As an initial value, we set $W^{(0)}(v_i^{(0)})$ to be equal to $W(v_i)$. The transfer matrix for the total value of arrows N is composed as

$$\begin{aligned} T_N^{(r)}(\eta_1, \beta_2, \eta_3, \beta_4 | \xi_1, \delta_2, \xi_3, \delta_4) \\ = \sum_{\alpha_1, \dots, \alpha_4} W^{(r)}(v_1^{(r)}(\alpha_1, \eta_1, \alpha_2, \xi_1)) \\ \times W(v_2(\alpha_2, \beta_2, \alpha_3, \delta_2)) W^{(r)}(v_3^{(r)}(\alpha_3, \eta_3, \alpha_4, \xi_3)) \\ \times W(v_4(\alpha_4, \beta_4, \alpha_1, \delta_4)), \end{aligned} \quad (12)$$

(see Fig. 4), where the total value of arrows N is obtained by

$$N = N_r(\eta_1) + \beta_2 + N_r(\eta_3) + \beta_4 = N_r(\xi_1) + \delta_2 + N_r(\xi_3) + \delta_4. \quad (13)$$

We denote arrows for a vertical bond at a renormalized vertex as ξ_i or η_i . The value of arrows included in the renormalized vertex is denoted by $N_r(\xi_i)$ for ξ_i or $N_r(\eta_i)$ for η_i ; $N_r(\xi_i)$ and $N_r(\eta_i)$ are equal to δ_i and β_i at the initial step of the DMRG procedure.

We denote an eigenvector of this transfer matrix by $\psi_{N,k}^{(r)}(\eta_1, \beta_2, \eta_3, \beta_4)$, which corresponds to the k th eigenvalue. As the usual DMRG method, we construct the density matrix $\hat{\rho}_{N,k}^{(r)}$ as

$$\begin{aligned} \rho_{N_r(\eta_1) + \beta_2, k}^{(r)}(\eta_1, \beta_2 | \xi_1, \delta_2) \equiv \sum_{\eta_3, \beta_4} \psi_{N,k}^{(r)}(\eta_1, \beta_2, \eta_3, \beta_4) \\ \times \psi_{N,k}^{(r)}(\xi_1, \delta_2, \eta_3, \beta_4). \end{aligned} \quad (14)$$

Notice that the density matrix is labeled by $N_r(\eta_1) + \beta_2$, not by N . This is due to the fact that η_3 and β_4 are shared by two eigenvectors constructing the density matrix, as shown in Fig. 5. From Eq. (13) we obtain $N_r(\eta_1) + \beta_2 = N_r(\xi_1) + \delta_2$ and therefore the density matrix has a block-diagonal form, as well as the transfer matrix, where each block is classified by the total value of arrows for the half system. This property of the density matrix is the reason why we can reduce the dimension of the transfer matrix by our method introduced in the present study.

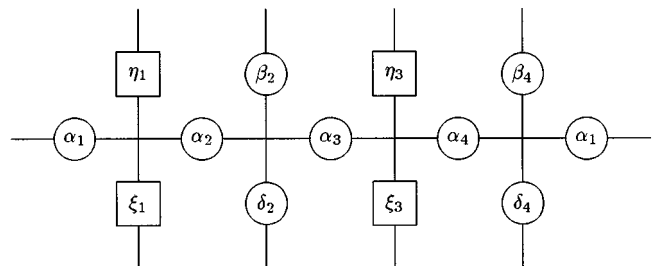


FIG. 4. Transfer matrix composed of weights W and $W^{(r)}$.

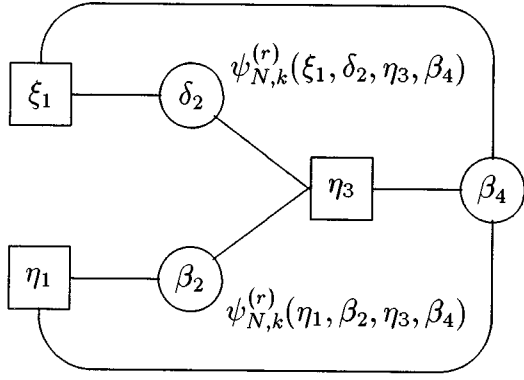


FIG. 5. Construction of the density matrix by a target state $\tilde{\psi}_{N,k}^{(r)}$ of the system. η_3 and β_4 are shared by two eigenvectors. Therefore, we obtain a conservation rule $N_r(\eta_1) + \beta_2 = N_r(\xi_1) + \delta_2$.

In order to construct the renormalized vertex weight $W^{(r+1)}$, we diagonalize the density matrix $\hat{\rho}_{N_r(\eta_1)+\beta_2,1}$ and obtain its eigenvectors $\vec{V}_{N_r(\eta_1)+\beta_2, \eta'_1}$. In the present study we use an eigenvector of the transfer matrix for the largest eigenvalue $k=1$ as a target state. The renormalized vertex state is labeled by η'_1 , which means that $\vec{V}_{N_r(\eta_1)+\beta_2, \eta'_1}$ corresponds to the η'_1 th eigenvalue of $\hat{\rho}_{N_r(\eta_1)+\beta_2,1}$. We determine the upper limit l of η'_1 as

$$l \equiv \begin{cases} 3^{r+2} & (3^{r+2} < m) \\ m & (3^{r+2} \geq m), \end{cases} \quad (15)$$

where m is the number of states taken into account for calculation of the density matrix. For example, at the initial step of the DMRG method, that is, $r=0$, the value of l becomes 9, which means that the renormalized arrow η'_1 includes two arrows.

The last step of the DMRG method for the 19-vertex model is the construction of the renormalized weight for the vertex as

$$\begin{aligned} & W^{(r+1)}(v_1^{(r+1)}(\alpha_1, \eta'_1, \alpha_3, \xi'_1)) \\ &= \sum_{\alpha_2} \sum_{\eta_1, \beta_2} \sum_{\xi_1, \delta_2} V_{N_r(\eta_1)+\beta_2, \eta'_1}(\eta_1, \beta_2) \\ & \quad \times W^{(r)}(v_1^{(r)}(\alpha_1, \eta_1, \alpha_2, \xi_1)) W(v_2(\alpha_2, \beta_2, \alpha_3, \delta_2)) \\ & \quad \times V_{N_r(\xi_1)+\delta_2, \xi'_1}(\xi_1, \delta_2). \end{aligned} \quad (16)$$

This last step is illustrated in Fig. 6. The total value of arrows included in the renormalized vertex becomes

$$N_{r+1}(\eta'_1) = N_r(\eta_1) + \beta_2. \quad (17)$$

We need also $W^{(r+1)}(v_3^{(r+1)}(\alpha_3, \eta'_3, \alpha_4, \xi'_3))$ when we return to the first step of the DMRG method, but we do not need to calculate it. Since in our method for the 19-vertex model the system has a translational symmetry, we can use $W^{(r+1)}(v_1^{(r+1)})$ as $W^{(r+1)}(v_3^{(r+1)})$. Then we return to the first step represented by Eq. (12) in order to iterate the DMRG procedure. By iterating this procedure for the 19-

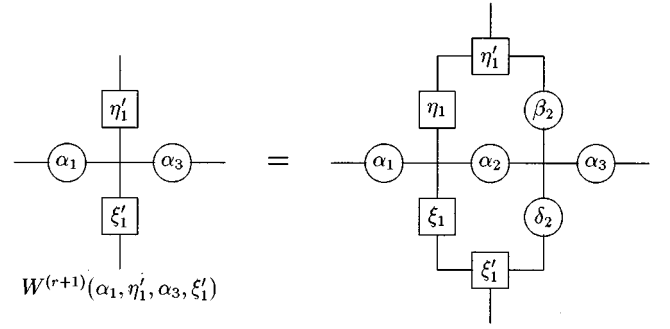


FIG. 6. Reconstruction of $W^{(r)}$ in terms of eigenvectors of the density matrix with restriction of the value of arrows.

vertex model with the restriction of the total value of arrows as mentioned above, we are able to make the system size L increase systematically. The advantage of this method is that the dimension of the transfer matrix decreases enormously by considering the conservation law of the value of arrows in this DMRG method. However, we need a large enough value of m in Eq. (15) in order to obtain a good accuracy of numerical calculations for a large system size. The results for the m dependence of the present method for the BKT transition are discussed in the following section, along with the other results obtained.

IV. RESULTS FOR THE CONFORMAL ANOMALY AND THE SMALLEST SCALING DIMENSION

An example of the values of $N_r(\eta_i)$ in the case of $m=35$, $N=0$, and $L=12$ is shown in Table I. The values of η_i in Table I are put in order according to the magnitude of the eigenvalues of the density matrix. Because the width of this system L is 12, η_i represents five arrows. Therefore, the value of $N_r(\eta_i)$ can take one of $\{-5, -4, \dots, 0, \dots, +4, +5\}$, as listed in the first column of Table I. Since we set $m=35$, there is no eigenvalue of the density matrix with $N_r(\eta_i) = \pm 5$. The crosses denote that there is no eigenvalue of η_i greater than 35. When the value of arrows is -4 , we have only one eigenvalue, which is the 31st eigenvalue of the density matrix. This is expressed as $N_r(31) = -4$ in the third

TABLE I. Example of the $N_r(\eta_i)$ structure in the case of $m=35$, $N=0$, and $L=12$. The crosses denote that there is no eigenvalue of η_i greater than 35.

$N_r(\eta_i)$	η_i						
-5	×	×	×	×	×	×	×
-4	31	×	×	×	×	×	×
-3	12	26	×	×	×	×	×
-2	4	11	19	28	×	×	×
-1	2	8	15	17	23	33	34
0	1	6	9	14	21	22	29
+1	3	7	16	18	24	32	35
+2	5	10	20	27	×	×	×
+3	13	25	×	×	×	×	×
+4	30	×	×	×	×	×	×
+5	×	×	×	×	×	×	×

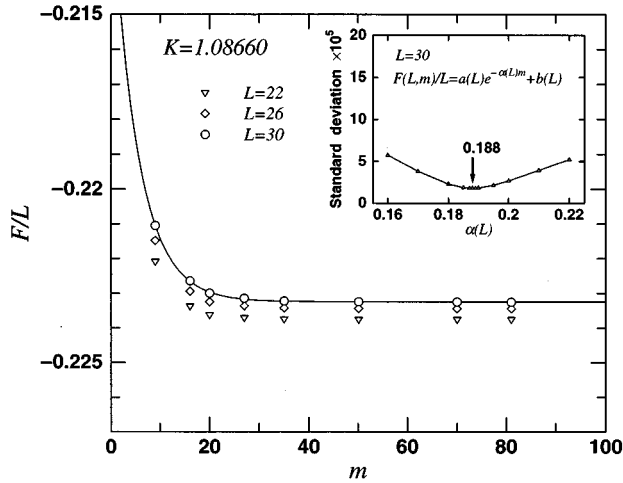


FIG. 7. m dependence of the free energy obtained by our method. We use three kinds of fitting functions and obtain the smallest standard deviation by an exponential function.

row of Table I. In the same way as for $N_r(\eta_i) = -4$, we have two eigenvalues with $N_r(\eta_i) = -3$: $N_r(12) = -3$ and $N_r(26) = -3$, as shown in the fourth row of Table I. For other values of $N_r(\eta_i)$, a distribution of η_i is shown in the same manner explained for $N_r(\eta_i) = -5$, $N_r(\eta_i) = -4$, and $N_r(\eta_i) = -3$. The largest eigenvalue corresponds to $N_r(1) = 0$. For the case of $m = 35$ given in Table I, the smallest eigenvalue corresponds to $N_r(34) = +1$ and $N_r(35) = -1$. These two states are degenerate. In general those two states with $N_r(\eta_i) \neq 0$ are degenerate; we have an eigenstate with $N_r(\eta_i)$ and an eigenstate with $-N_r(\eta_i)$ always. Therefore, an eigenstate distribution of the density matrix is symmetric with respect to $N_r(\eta_i)$.

The dimension of a matrix that has to be diagonalized in the DMRG method is now enormously reduced by the method mentioned in Sec. III. Therefore, it becomes possible to handle large values of m by using our computer resources. As an example we show a reduction of the dimension of matrices of which the largest eigenvalues have to be calculated. In the case of $N=0$, $m=35$, and $L=12$, the dimension of a matrix is $3^{12} = 531\,441$ for a simple transfer matrix method. The dimension of the matrix reduces down to $(35 \times 3)^2 = 11\,025$ for the usual DMRG method [1,2]. The dimension of the matrix is now 1545 for our method introduced in the present study.

The largest eigenvalue of the transfer matrix belongs to the block with $N=0$ in the whole transfer matrix. Hence the largest eigenvalue with $N=0$ is used to calculate the free energy of the system. The m dependence of the value of the free energy is shown in Fig. 7. We obtain a good convergence with the value of m . In the case of $L=30$, calculations with $m = 3^{14} = 4\,782\,969$ give an exact diagonalization of the transfer matrix. Three kinds of fitting functions are used to fit the m dependence. We obtain the smallest value of standard deviation by using an exponential function. These results mean that the largest eigenvalue of the transfer matrix exponentially converges to an exact value by increasing m even at the BKT transition point in our method.

The size dependence of the free energy F at $K=1.0866$, which is regarded as the BKT transition point by Knops

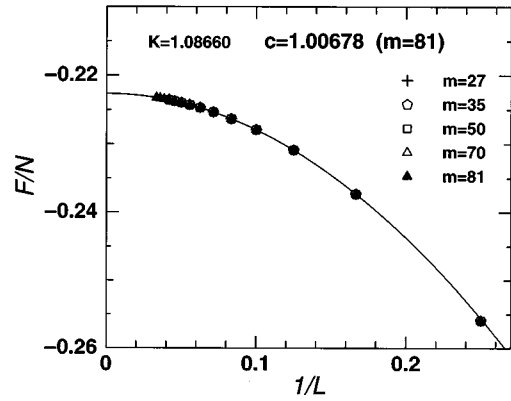


FIG. 8. Size dependence of the free energy of the 19-vertex model at $K=1.0866$. The estimated value of the conformal anomaly from this result is $c=1.006(1)$.

et al. [3], is shown in Fig. 8. We use the following size dependence [11] of the free energy for the system with periodic boundary conditions:

$$F/L \sim f_\infty - \frac{\pi c}{6L^2}, \quad (18)$$

where f_∞ denotes the free energy per site in the thermodynamic limit. We obtain the value of the conformal anomaly as $c=1.006(1)$, which is consistent with the value of c at the critical region.

The second largest eigenvalue of the transfer matrix belongs to a block with $N=1$. Hence the smallest scaling dimension that is equivalent to $\eta/2$ is estimated by

$$\eta/2 = x_0^{(1)} = \frac{L}{2\pi} \ln \left(\frac{\lambda_0^{(0)}}{\lambda_0^{(1)}} \right), \quad (19)$$

where $\lambda_k^{(n)}$ expresses the k th eigenvalue in the $N=n$ sector of the transfer matrix [3]. The critical index η describes an algebraic decay of a correlation function in a critical region of interaction. At the BKT transition point, the value of η has to be $\frac{1}{4}$. An interaction dependence of $x_0^{(1)}$ is shown in Fig. 9. The results shown in Fig. 9 are obtained by using

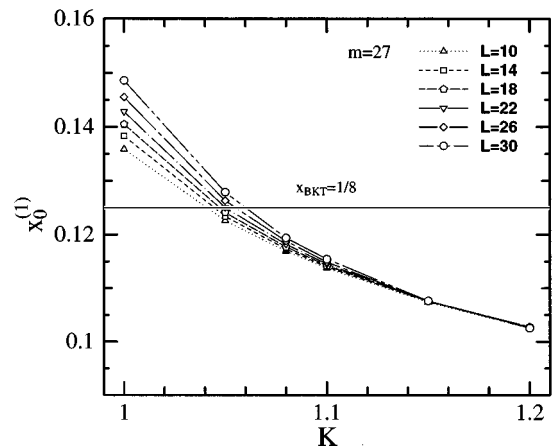


FIG. 9. Interaction dependence of the smallest scaling dimension $x_0^{(1)}$.

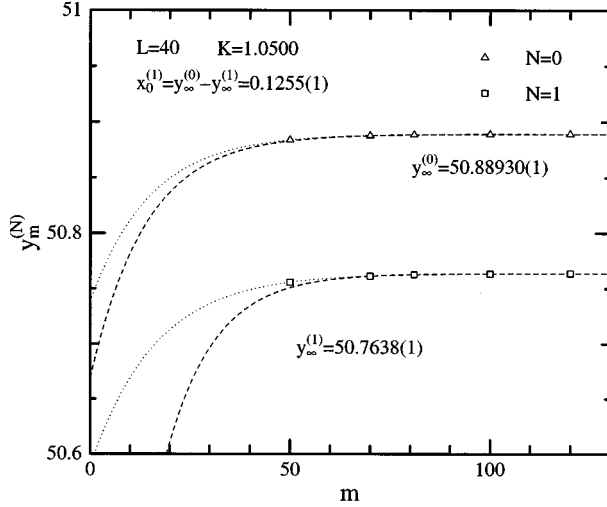


FIG. 10. m dependences of $y_m^{(N)}$ at $K=1.0500$ for $L=40$.

$m=27$ for each L . In Fig. 9 we fail to obtain the value $\frac{1}{8}$ of $x_0^{(1)}$ if we use $K=1.0866$: The value of $\eta/2$ obviously appears to be smaller than $1/8$ at $K=1.0866$.

We investigate an m dependence of $x_0^{(1)}$ at $K=1.0866$ and $K=1.0500$ up to $m=120$. Examples of extrapolations to large values of m by using the exponential function are shown in Fig. 10. We define $y_m^{(N)}$ by

$$y_m^{(N)} \equiv \frac{L}{2\pi} \ln \lambda_{0,m}^{(N)}, \quad (20)$$

where $\lambda_{0,m}^{(N)}$ is the largest eigenvalue of the transfer matrix with the value of arrows N constructed by taking account of m states of the density matrix. In order to obtain results that are equivalent to an exact diagonalization, we need a large value of m , i.e., $m=3^{19}$, for the largest system size $L=40$, which we treat. Therefore, we extrapolate the obtained results $y_m^{(N)}$ to $m=\infty$ in Fig. 10. In Fig. 10 dashed lines are the results of fitting by using values obtained from $m=70, 81, 100,$ and 120 . The dotted lines are results of fitting by using values from $m=50, 70, 81, 100,$ and 120 . The difference between the results obtained from these two extrapolations is shown as errors in Fig. 10. We evaluate the value of $x_0^{(1)}$ by $y_\infty^{(0)} - y_\infty^{(1)}$ and obtain the value $x_0^{(1)}=0.1255(1)$ at $K=1.0500$ for $L=40$.

In Figs. 11 and 12 we show the size dependences of $x_0^{(1)}$ at $K=1.0866$ and $K=1.0500$, respectively. All points shown in Figs. 11 and 12 are values estimated from extrapolations of m as explained above. We observe that the value of $x_0^{(1)}$ goes to a finite value for large L . The extrapolated value is about 0.1175 and obviously less than $1/8$ at $K=1.0866$. Therefore, $K=1.0866$ is in the critical region. On the other hand, it is found that the size dependence of $x_0^{(1)}$ at $K=1.0500$ is stronger than that at $K=1.0866$, as shown in Fig. 12. In addition, the value of $x_0^{(1)}$ increases beyond $1/8$ as the system size L increases. This result indicates that $K=1.0500$ is out of the critical region.

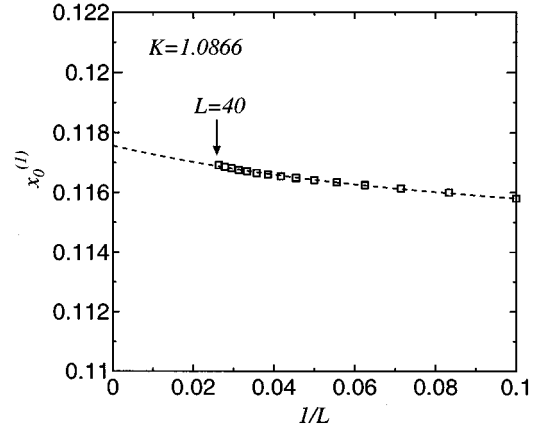


FIG. 11. Size dependence of $x_0^{(1)} = \eta/2$ at $K=1.0866$. The value of $x_0^{(1)}$ is expected to be $0.1175(5)$ for large L , which is obviously below the $1/8$ expected for the BKT transition point. The dashed line is just a guide for the eye.

Thus these results at $K=1.0866$ and $K=1.0500$ suggest that the critical value of K of the 19-vertex model is between $K=1.0500$ and $K=1.0866$. The determination of a precise value of the critical point K_c is an interesting problem. However, this problem is beyond the purpose of the present study. A further investigation for this point is left as a future problem.

V. SUMMARY

We have succeeded in reducing enormously the dimension of the matrix to be diagonalized in the DMRG method for the 19-vertex model by using the ice rule. It has been found that the m dependence of the free energy shows an exponential convergence even near the BKT transition point by using our method. An accurate result is obtained for the conformal anomaly, i.e., $c=1.006(1)$ near the BKT transition point, by means of the present approach.

From the size dependence of the smallest scaling dimension $x_0^{(1)}$ ($=\eta/2$) we have found that $K=1.0866$ belongs to

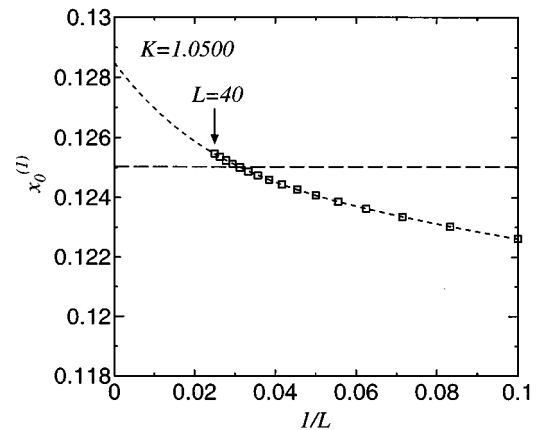


FIG. 12. Size dependence of $x_0^{(1)} = \eta/2$ at $K=1.0500$. We observe a stronger size dependence than that at $K=1.0866$ and find that the value is beyond $1/8$. The dashed line is just a guide for the eye.

the critical region. However, the estimated value of $\eta/2$ is smaller than $1/8$. On the other hand, our results for $K=1.0500$ suggest that the value of $\eta/2$ is larger than $1/8$. These results mean that the critical point of the 19-vertex model is between $K=1.0500$ and $K=1.0866$. A further investigation for this point is left as a future problem.

ACKNOWLEDGMENTS

This work was partially supported by a Grant-In-Aid for Scientific Research from the Ministry of Education, Science and Culture, Japan and also by the Computer Center of Tohoku University.

-
- [1] S. R. White, Phys. Rev. Lett. **69**, 2863 (1992); Phys. Rev. B **48**, 10 345 (1993).
[2] T. Nishino, J. Phys. Soc. Jpn. **64**, 3598 (1995).
[3] Y. M. M. Knops, B. Nienhuis, H. J. F. Knops, and H. W. J. Blöte, Phys. Rev. B **50**, 1061 (1994).
[4] A. B. Zamolodchikov and Fateev, Sov. J. Nucl. Phys. **32**, 298 (1980).
[5] K. Sogo, Y. Akutsu, and T. Abe, Prog. Theor. Phys. **70**, 730 (1983).
[6] K. Sogo, Y. Akutsu, and T. Abe, Prog. Theor. Phys. **70**, 739 (1983).
[7] V. L. Berezinskii, Zh. Éksp. Teor. Fiz. **59**, 907 (1970) [Sov. Phys. JETP **32**, 493 (1971)].
[8] J. M. Kosterlitz and D. J. Thouless, J. Phys. C **6**, 1181 (1973).
[9] J. M. Kosterlitz, J. Phys. C **7**, 1046 (1974).
[10] R. J. Baxter, *Exactly Solved Models in Statistical Mechanics* (Academic, London, 1982), Chap. 8 and references cited therein.
[11] H. W. J. Blöte, J. L. Cardy, and M. P. Nightingale, Phys. Rev. Lett. **56**, 742 (1986).